

# Origin of temperature and field dependence of magnetic skyrmion size in ultrathin nanodots

R. Tomasello<sup>1</sup>, K. Y. Guslienko<sup>2,3</sup>, M. Ricci<sup>4</sup>, A. Giordano<sup>5</sup>, J. Barker<sup>6</sup>, M. Carpentieri<sup>7</sup>,  
O. Chubykalo-Fesenko<sup>8</sup>, G. Finocchio<sup>5</sup>

<sup>1</sup> *Dept. Engineering, Polo Scientifico Didattico di Terni, University of Perugia, 50100 Terni, Italy*

<sup>2</sup> *Depto. Física de Materiales, Universidad del País Vasco, UPV/EHU, 20018 San Sebastián, Spain*

<sup>3</sup> *IKERBASQUE, the Basque Foundation for Science, 48013 Bilbao, Spain*

<sup>4</sup> *Dept. Computer Science, Modeling, Electronics and System Science, University of Calabria, I-87036 Rende, Italy*

<sup>5</sup> *Dept. Mathematical and Computer Sciences, Physical Sciences and Earth Sciences, University of Messina, 98166 Messina, Italy*

<sup>6</sup> *Institute for Materials Research, Tohoku University, 980-8577 Sendai, Japan*

<sup>7</sup> *Dept. Electrical and Information Engineering, Politecnico di Bari, 70125 Bari, Italy*

<sup>8</sup> *Instituto de Ciencia de Materiales de Madrid, CSIC, Cantoblanco, 28049 Madrid, Spain*

Understanding the physical properties of magnetic skyrmions is important for fundamental research with the aim to develop new spintronic device paradigms where both logic and memory can be integrated at the same level. Here, we show a universal model based on the micromagnetic formalism that can be used to study skyrmion stability as a function of field and temperature. We consider ultrathin, circular magnetic dots. Our results show that magnetic skyrmions with a small radius compared with the dot radius are always metastable, but large radius skyrmions occupy a stable ground state stabilized by the confining potential. This energy profile determines the weak (strong) temperature size dependence of the metastable (stable) skyrmion as a function of the temperature. Those results can open a path toward the design of efficient materials for skyrmion based devices.

Non-linear localized excitations have attracted the attention of physicists for a long time. Such excitations, including solitary waves or solitons, play important role in optics, quantum field theory, condensed matter, etc. Sometimes it is possible to associate integer numbers (topological charges) to the solitons, which are preserved in their dynamics. Topologically non-trivial magnetization configurations in ferromagnets, such as domain walls, vortices, and skyrmions are currently the focus of a lot of research activity, and are also candidates for several nanoscale device applications (computational paradigms, magnetic storage and programmable logic) due to their small size [1–14].

Skyrmion solutions were obtained first by Skyrme in the non-linear field theory [15,16], and, subsequently discovered experimentally in non-centrosymmetric B20 compounds [17–20] allowing for an asymmetric Dzyaloshinskii-Moriya spin-spin exchange interaction (DMI) [21,22]. Recent efforts have been focusing on materials with interfacial DMI, especially ultra-thin transition metal/heavy metal multilayers with large spin-orbit coupling such as Co/Pt and Co/Ir [8,23,24]. It is accepted that DMI is crucial for the skyrmion stabilization in ultrathin magnetic elements and the skyrmions can be further stabilized by external fields [8,23,24]. Temperature is usually considered to be a detrimental factor leading either to the transformation of the skyrmion state into a more energetically favourable state [25] or to the nucleation of multiple skyrmions and labyrinth domains [8,23,24].

Recently, Rohart *et al.* [26] developed a domain wall model of the Néel skyrmions at both zero temperature  $T$  and magnetic field  $H_{ext}$  and identified a critical DMI parameter  $D_c$  serving as a scale to quantify the influence of DMI that does not depend on the dot size. They found that the single skyrmion is metastable for the absolute values of the DMI parameter  $D$  lower than  $D_c$  and does not exist if  $D > D_c = (4/\pi)\sqrt{AK_{eff}}$ , where  $A$  and  $K_{eff}$  are the exchange stiffness and effective uniaxial magnetic anisotropy constants. The skyrmion radius  $R_{sk}$  diverges for  $D \rightarrow D_c$  within their analytical model. However, in a finite magnetic dot,  $R_{sk}$  is determined by the confining potential and cannot exceed the dot radius  $R_d$  [26]. Therefore, the analytical model yields incorrect results at  $D > D_c$  and should be improved.

The temperature dependence of skyrmion radius in infinite film was calculated as a result of the temperature dependence of the magnetic properties of the host material by Barker *et al.* [27] using Rohart *et al.* [26] expression for  $R_{sk}$ . The bulk scaling relations of  $A$  and  $K_u$  with respect to the reduced magnetization  $m(T) = M_s(T)/M_s(0)$  were used ( $M_s$  is the saturation magnetization), while no temperature dependence of  $D$  was considered. The authors concluded that in

ferromagnets the skyrmion radius have weak quasi-linear temperature dependence. This is rather a result of using the Rohart's *et al.* equation for small radius ( $\sim 10$  nm) skyrmions that have a size comparable with the domain wall width.

Recent room-temperature experiments, where an external out-of-plane magnetic field was applied [8,23], showed a strong non-linear dependence of the skyrmion radius on the external field strength. The main motivation of this work is related to the fact that currently, there is no comprehensive analytical theory of the skyrmion stability and size calculated from the magnetic and geometric parameters of a finite sample including influence of temperature and external magnetic field.

Here, we develop a theoretical approach to the skyrmion stability based on minimization of the magnetic energy using a skyrmion ansatz in confined geometries. We show that temperature evolution of the skyrmion size in ultrathin dots is determined by proximity of the point describing the skyrmion state in a  $Q$ - $d$  phase space to a border of the skyrmion stability. The key dimensionless parameters determining the skyrmion stability and size are the quality factor  $Q = 2K_u/\mu_0 M_s^2$ , and the reduced DMI strength  $d = |D|l_{ex}/A$  ( $l_{ex} = \sqrt{2A/\mu_0 M_s^2}$  is the exchange length). The temperature dependence of the skyrmion stability is taken into account by considering the scaling relations of both  $Q$  and  $d$  with  $T$ . We show that the equilibrium skyrmion size increases drastically with temperature increasing only approaching a critical line  $d_c(Q) = (4/\pi)\sqrt{Q-1}$  and reaches large values comparable with the dot radius at  $d(T) > d_c(T)$ . The metastable skyrmions have small radius ( $R_{sk} \ll R_d$ ), whereas the stable (ground state) ones have large radius. The out-of-plane external magnetic field can be used to bring the metastable skyrmions closer or farther away from the critical line  $d_c(Q)$  where the metastable skyrmion becomes a ground state skyrmion.

Seeking a general expression for the skyrmion size dependence on both temperature and external magnetic field, we developed an analytical approach using a skyrmion ansatz different from Ref. [26], but useful to that overcome drawbacks of previous approaches in estimating the skyrmion radius [28] (see note 1 in the Supplemental Material for the details of the analytical approach). We propose the following trial function to minimize the energy functional:

$$\tan \frac{\Theta_0(r)}{2} = \frac{r_{sk}}{r} e^{\xi(r_{sk}-r)} . \quad (1)$$

Then, the energy  $E$  and the equilibrium skyrmion radius  $r_{sk} = R_{sk} / l_{ex}$  can be expressed as functions  $E[r_{sk}, Q, d, H_{ext}]$  and  $r_{sk}[Q, d, H_{ext}]$ , and the conditions of the skyrmion stability can be found from the standard variational procedure solving the equations  $\partial E / \partial r_{sk} = 0$ ,  $\partial^2 E / \partial r_{sk}^2 = 0$ . To take into account the temperature dependence of the skyrmion diameter, we use the scaling approach for macroscopic (micromagnetic) parameters which decrease with temperature due to the magnetization fluctuation effects. The thermal micromagnetic approach is known to largely overestimate the Curie temperature as compared to the more accurate atomistic approach [29]. However, the largest temperatures considered in the present study are very far from the Curie temperature ( $T / T_c < 1/2$ ). In this case, the micromagnetic approach produces the correct results in terms of the thermodynamically averaged quantities as a function of magnetization  $m(T)$ . Specifically, for the temperature dependence of uniaxial magnetic anisotropy we expect to obtain the Callen-Callen relation  $K_u(T) = K_u(0)m(T)^{3.03}$  [30]. Whereas, the scaling of the exchange parameter  $A(m) = A(0)m^\alpha$  and DMI  $D(T) = D(0)m(T)^\beta$  are found by atomistic simulations calculating the thermal spin wave spectrum and fitting the long wavelength regime (small  $\mathbf{k}$ -vectors) with a linear spin wave theory [28] (see note 2 in the Supplemental Material). We obtain  $\alpha = \beta = 1.5$ , consistently with recent calculations [31,32].

In order to benchmark the theory, we consider a circular nanodot (e.g., Co) of diameter  $2R_d = 400$  nm and thickness of 0.8 nm and assume that it is in contact with a thin heavy metal layer (e.g., Pt) giving an appreciable interfacial DMI. We have performed systematic micromagnetic simulations of the skyrmion diameter as a function of the out-of-plane external field  $H_{ext}$  (from 0 mT to 50 mT) and temperature (from 0 K to 300 K) integrating the Landau-Lifshitz-Gilbert equation of motion for the reduced magnetization  $\mathbf{m} = \mathbf{M} / M_s$  [28] (see note 3 in the Supplemental Material). At  $T=0$  K, we used the following material parameters:  $M_s = 600$  kA/m [8],  $A = 20$  pJ/m [33],  $D = 3.0$  mJ/m<sup>2</sup> [34,35],  $K_u = 0.60$  MJ/m<sup>3</sup> [8], and Gilbert damping  $\alpha_G = 0.1$  [36]. While comparing our results, we consider, as a reference, the critical DMI value  $D_c = 3.48$  mJ/m<sup>2</sup> for our parameters at  $T=0$  K [26].

Temperature causes the skyrmion to diffuse and leads to fluctuations of the diameter and deformations of the skyrmion shape [27,37,38], which then loses the circular symmetry. Therefore, we calculated the diameter assuming that the area of the skyrmion core is equivalent to a circle [27]. The skyrmion diameter and perimeter display approximately Gaussian statistical distributions

[28] (see note 3 in the Supplemental Material) with temperature-increased widths. The application of the magnetic field significantly decreases both mean and standard deviation of the distribution.

The dependence of the skyrmion size on the magnetic field calculated by using the skyrmion ansatz, Eq. (1), at  $T=0$  K is presented in Fig. 1(a). There is a good agreement between the analytical calculations and micromagnetic simulations, without any fitting parameter. Fig. 1(b) shows the dependence of the skyrmion diameter on temperature for three values of the external field, as obtained by micromagnetic simulations (open symbols). At zero field, the skyrmion diameter strongly increases with temperature increasing. The increase of the out-of-plane field results in a weak quasi-linear increasing of the diameter up to  $T=300$  K (red circles and green triangles in Fig. 1(b)). Our computations show that two thermal/field regimes exist: at high temperature ( $T>200$  K) and low field ( $H_{ext}<10$  mT), the skyrmion size is strongly influenced by thermal fluctuations, whereas at low temperature ( $T\leq 200$  K) independently of the field, or at high temperature and high field ( $H_{ext}\geq 10$  mT), the skyrmion is weakly affected by thermal fluctuations. Those different behaviors were not observed in Ref. [30], because, for the parameters used in that paper, the skyrmion was always metastable. Now, considering the skyrmion diameter as a function of the external field for  $T=300$  K (Fig. 1(b)), it can be also noted a strong variation as the external field is reduced. Those data are consistent with experimental results in Refs. [8,23].

By including the scaling relations in the analytical approach as calculated from atomistic simulations, we find results in agreement with micromagnetic simulations until the skyrmion is in the metastable region far from the boundary of the stable region [28](e.g. when  $T<200$  K for  $H_{ext}=0$  mT, see note 3 in the Supplemental Material). While in the metastable region, the skyrmion size is mainly related to a trade-off among exchange, external field and DMI, when approaching the ground state region, the confining potential due to the magnetostatic field and the DMI boundary conditions start to play a significant role in fixing the skyrmion size [11,26], i.e. the skyrmion diameters depends on the dot size. In order to take into account this effect, we consider the scaling exponent  $\gamma$  of the uniaxial perpendicular anisotropy  $K_u(T)=K_u(0)m(T)^\gamma$  as fitting parameter. This is because the analytical model is developed within the thin-film approximation where the effective anisotropy is computed as  $K_{eff}(T)=K_u(T)-0.5\mu_0M_s(T)^2$ . By performing athermal (deterministic) micromagnetic simulations [28](see note 3 in the Supplemental Material), an excellent agreement is found for  $\gamma=3.585$ . With this value, we can calculate the skyrmion diameter dependence on temperature and field by Eq. (1) (dashed lines in Fig. 1(b)). The analytical and micromagnetic results agree well and we conclude that our analytical expression is accurate in predicting the skyrmion size for arbitrary temperature and external field combinations.

To understand the origin of the two thermal/field regimes, we focus on the data achieved at zero external field. We can calculate the critical DMI parameter for each set of scaled parameters by the expression  $D_c(T) = 4\sqrt{A(T) \cdot K_{\text{eff}}(T)}/\pi$  [29]. When  $D$  approaches  $D_c$  (as the temperature increases, see Fig. 2), a sharp increase of the skyrmion size  $R_{\text{sk}}(T)$  occurs [26]. This could explain why, at room temperature, the skyrmion size essentially increases for  $H_{\text{ext}} < 5$  mT exhibiting a non-linear dependence on the external field [8,23] (see note 3 in the Supplemental Material [28]).

The scaling of macroscopic parameters leads to the quality factor temperature dependence  $Q(T) = Q(0)m(T)$ . Accounting for the definition  $d(T) = D(T)l_{\text{ex}}(T)/A(T)$ , we can derive the temperature dependence of the reduced DMI parameter as  $d(T) = d(0)[m(T)]^{\beta-\alpha/2-1}$ . We note that temperature dependence of the reduced critical DMI parameter  $d_c(m) \propto m^{-1}\sqrt{K_{\text{eff}}(m)} \propto \sqrt{Q(m)-1}$  includes neither the exchange stiffness  $\alpha$  nor the DMI exponent  $\beta$ . This justifies the use of the skyrmion stability diagram in the reduced coordinates,  $Q$  and  $d$ , presented in Fig. 3(a). The parameters at  $T=0$  K are:  $Q(0)=2.65$ ,  $d(0)=1.41$ ,  $l_{\text{ex}}(0)=9.4$  nm, (the scaling law for the reduced DMI parameter is  $d(m) \propto m^{\beta-\alpha/2-1}$ , i.e.,  $d(m) \propto m^{-0.84}$ ). The dependence  $d(m)$  determines the evolution of the point describing the skyrmion configuration in the  $Q$ - $d$  plane accounting change of temperature via the  $m(T)$  law (Fig. 3(a)). The increase of parameter  $d$  leads to the stabilization of the skyrmion state and a drastic increase of the skyrmion radius. This effect is especially strong at  $H_{\text{ext}}=0$  mT. On the other hand, a finite value of the field  $H_{\text{ext}}$  directed opposite to the skyrmion core magnetization, results in shrinking of the skyrmion radius and, therefore, the skyrmion radius weakly increases with  $T$ . In other words, the skyrmion radius increase is not so drastic for finite magnetic field as it was for zero field.

We can state that there are two possible qualitatively different *scenarios* of the temperature dependence of the skyrmion radius  $R_{\text{sk}}(T)$  according to the parameters  $Q$  and  $d$ , as also observed in the micromagnetic simulations:

- 1) The skyrmion radius  $R_{\text{sk}}(T)$  sharply increases with temperature increasing when approaching the skyrmion stability region.
- 2) The skyrmion radius  $R_{\text{sk}}(T)$  is almost constant as a function of temperature when the skyrmion configuration remains metastable.

The first scenario is realized for the parameters  $Q(0)$ ,  $d(0)$ ,  $l_{\text{ex}}(0)$  corresponding to the skyrmion metastable state (see Figs. 3(a) and (b)). This is realized for our dot magnetic parameters,  $D < D_c$  from  $T=0$  K to  $T=350$  K (green points in Fig. 3 (a)). In this case, the skyrmion radius at  $T=0$  K is

small, but it reveals strong temperature dependence  $R_{sk}(T)$  with increasing temperature because the skyrmion moves from the metastable area towards the area of the global stability in  $Q$ - $d$  magnetic phase diagram. When increasing  $T$ , the skyrmion can reach the area of its stability (magenta point in Fig. 3(a)) or stay in a metastable state depending on the values of  $T$  and  $\beta$ . The value of the skyrmion radius  $R_{sk}(T, H_{ext})$  is also sensitive to the out-of-plane field  $H_{ext}$ . The increase of field suppresses the increase of the value of  $R_{sk}(T)$ . If we cross the uniform state-skyrmion equilibrium line (red dashed line in Fig. 3(a) where the skyrmion energy is equal to the perpendicular uniform state energy,  $d = d_c$ ), the skyrmion radius is large and the ratio  $R_{sk} / R$  is a weak function of all parameters.

The second scenario is realized for the parameters  $Q(0)$ ,  $d(0)$ ,  $l_{ex}(0)$  corresponding to the skyrmion ground state (Figs. 3(a) and (c)). In this case, the skyrmion radius at  $T=0$  K is large and it reveals only weak temperature dependence  $R_{sk}(T)$  because the skyrmion state is already in the area of its stability in  $Q$ - $d$  magnetic phase diagram. In particular, the skyrmion radius calculated by means of deterministic micromagnetic simulations with scaled values of the parameters ( $T=400$  K) is much larger than the skyrmion radius for  $T=300$  K (compare spatial distribution of the magnetization in Fig. 3(b) with the one in Fig. 3(c)). In addition, when thermal fluctuations are considered in the micromagnetic simulations, we observe strong deformations of the skyrmion for  $T=400$  K, which turns into a “horseshoe”-like configuration as already observed in experiments [8], while it remains quasi-circular for  $T=300$  K (see insets in Fig. 3(a)). The skyrmion radius is large and the ratio  $R_{sk} / R_d$  is a weak function of all parameters. The decreasing function  $d(m)$  guarantees that the skyrmion state is in the  $(Q, d)$ -area of the skyrmion stability at temperature increasing. We do not consider here stabilization of multiple skyrmions or labyrinth domain textures assuming that the parameter  $d$  is not very large and we are always in the area of the single skyrmion stability.

This fundamental finding can be used to appropriately design skyrmion based devices. Fig. 4 shows an example for the electrical detection [38] of skyrmions in racetrack memory. The green square represents a magnetic tunnel junction (MTJ) with a polarized designed properly in order to generate a dipolar coupling that can modify the stability properties of the skyrmion below the contact itself. In other words, skyrmions are metastable while shifted in the track (the smaller the skyrmions are, the higher the storage density is), whereas they become quasi-stable below the MTJ to enhance their detection via the tunnelmagnetoresistance signal (see Supplemental Material Video 1 [28]).

In summary, we have developed a theoretical framework for the description of skyrmion stability as a function of the external field and temperature by combining a proper ansatz and the thermal dependence included through the scaling relations of the micromagnetic parameters  $A$ ,  $K_u$  and  $D$  with magnetization. We have shown that the strong temperature dependence of the skyrmion diameter is a result of the fact that the initially metastable skyrmion in the process of thermal evolution approaches the ground state region where the skyrmion energy is essentially reduced due to increase of the DMI strength. Our results, corroborated by extensive micromagnetic simulations, provide a tool to study the transition from metastable to ground state skyrmion as well as the skyrmion size in presence of both out-of-plane external field and temperature. In addition, our achievements can drive the design of racetrack memories for an efficient manipulation of skyrmions, where, for example, local variation of some parameters can be used to vary the skyrmion stability thus improving the possibility for the electrical detection.

## ACKNOWLEDGMENTS

This work was supported by the program of scientific and technological cooperation between Italy and China (code CN16GR09) funded by Ministero degli Affari Esteri e della Cooperazione Internazionale, and by the bilateral Italy-Turkey project (CNR Grant #: B52I14002910005, TUBITAK Grant # 113F378). R.T. and M.R. thank Fondazione Carit Projects ‘Sistemi Phased-Array Ultrasonori’, and ‘Sensori Spintronici’. K.G. acknowledges support by IKERBASQUE (the Basque Foundation for Science). The work of K.G. and O.C.-F. was supported by the Spanish Ministry of Economy and Competitiveness under projects MAT2013-47078-C2-1-P, MAT2013-47078-C2-2-P and FIS2016-78591-C3-3-R. J.B. acknowledges support from the Graduate Program in Spintronics, Tohoku University.

## References

- [1] S. Emori, U. Bauer, S.-M. Ahn, E. Martinez, and G. S. D. Beach, *Nat. Mater.* **12**, 611 (2013).
- [2] K. S. Ryu, L. Thomas, S.-H. Yang, and S. S. P. Parkin, *Nat. Nanotechnol.* **8**, 527 (2013).
- [3] S. Parkin and S.-H. Yang, *Nat. Nanotechnol.* **10**, 195 (2015).
- [4] K. S. Buchanan, P. E. Roy, F. Y. Fradin, K. Y. Guslienko, M. Grimsditch, S. D. Bader, and V. Novosad, *J. Appl. Phys.* **99**, 08C707 (2006).
- [5] G. Siracusano, R. Tomasello, A. Giordano, V. Puliafito, B. Azzerboni, O. Ozatay, M. Carpentieri, and G. Finocchio, *Phys. Rev. Lett.* **117**, 87204 (2016).
- [6] J. Sampaio, V. Cros, S. Rohart, A. Thiaville, and A. Fert, *Nat. Nanotechnol.* **8**, 839 (2013).
- [7] R. Tomasello, E. Martinez, R. Zivieri, L. Torres, M. Carpentieri, and G. Finocchio, *Sci. Rep.* **4**, 6784 (2014).
- [8] S. Woo, K. Litzius, B. Krüger, M.-Y. Im, L. Caretta, K. Richter, M. Mann, A. Krone, R. M. Reeve, M. Weigand, P. Agrawal, I. Lemesh, M.-A. Mawass, P. Fischer, M. Kläui, and G. S. D. Beach, *Nat. Mater.* **15**, 501 (2016).
- [9] G. Finocchio, F. Büttner, R. Tomasello, M. Carpentieri, and M. Kläui, *J. Phys. D. Appl. Phys.* **49**, 423001 (2016).
- [10] W. Jiang, W. Zhang, G. Yu, M. B. Jungfleisch, P. Upadhyaya, H. Somaily, J. E. Pearson, Y. Tserkovnyak, K. L. Wang, O. Heinonen, S. G. E. te Velthuis, and A. Hoffmann, *AIP Adv.* **6**, 55602 (2016).
- [11] G. Finocchio, M. Ricci, R. Tomasello, A. Giordano, M. Lanuzza, V. Puliafito, P. Burrascano, B. Azzerboni, and M. Carpentieri, *Appl. Phys. Lett.* **107**, 262401 (2015).
- [12] R. H. Liu, W. L. Lim, and S. Urazhdin, *Phys. Rev. Lett.* **114**, 137201 (2015).
- [13] Y. Zhou, E. Iacocca, A. A. Awad, R. K. Dumas, F. C. Zhang, H. B. Braun, and J. Åkerman, *Nat. Commun.* **6**, 8193 (2015).
- [14] M. Carpentieri, R. Tomasello, R. Zivieri, and G. Finocchio, *Sci. Rep.* **5**, 16184 (2015).
- [15] T. H. R. Skyrme, *Nucl. Phys.* **31**, 556 (1962).
- [16] A. N. Bogdanov and U. K. Rößler, *Phys. Rev. Lett.* **87**, 37203 (2001).
- [17] S. Muhlbauer, B. Binz, F. Jonietz, C. Pfleiderer, A. Rosch, A. Neubauer, R. Georgii, and P. Boni, *Science* **323**, 915 (2009).
- [18] A. Neubauer, C. Pfleiderer, B. Binz, A. Rosch, R. Ritz, P. G. Niklowitz, and P. Böni, *Phys. Rev. Lett.* **102**, 186602 (2009).
- [19] S. X. Huang and C. L. Chien, *Phys. Rev. Lett.* **108**, 267201 (2012).
- [20] M. C. Langner, S. Roy, S. K. Mishra, J. C. T. Lee, X. W. Shi, M. A. Hossain, Y.-D. Chuang, S. Seki, Y. Tokura, S. D. Kevan, and R. W. Schoenlein, *Phys. Rev. Lett.* **112**, 167202 (2014).

- [21] I. Dzyaloshinsky, *J. Phys. Chem. Solids* **4**, 241 (1958).
- [22] T. Moriya, *Phys. Rev. Lett.* **4**, 4 (1960).
- [23] C. Moreau-Luchaire, C. Moutafis, N. Reyren, J. Sampaio, C. A. F. Vaz, N. Van Horne, K. Bouzehouane, K. Garcia, C. Deranlot, P. Warnicke, P. Wohlhüter, J.-M. George, M. Weigand, J. Raabe, V. Cros, and A. Fert, *Nat. Nanotechnol.* **11**, 444 (2016).
- [24] O. Boulle, J. Vogel, H. Yang, S. Pizzini, D. de S. Chaves, A. Locatelli, T. O. M. A. Sala, L. D. Buda-Prejbeanu, O. Klein, M. Belmeguenai, Y. Roussigné, A. Stashkevich, S. M. Chérif, L. Aballe, M. Foerster, M. Chshiev, S. Auffret, I. M. Miron, and G. Gaudin, *Nat. Nanotechnol.* **11**, 449 (2016).
- [25] S. Rohart, J. Miltat, and A. Thiaville, *Phys. Rev. B* **93**, 214412 (2016).
- [26] S. Rohart and A. Thiaville, *Phys. Rev. B* **88**, 184422 (2013).
- [27] J. Barker and O. A. Tretiakov, *Phys. Rev. Lett.* **116**, 147203 (2016).
- [28] Supplemental Material can be found at [ ].
- [29] G. Grinstein and R. H. Koch, *Phys. Rev. Lett.* **90**, 207201 (2003).
- [30] P. Asselin, R. F. L. Evans, J. Barker, R. W. Chantrell, R. Yanes, O. Chubykalo-Fesenko, D. Hinzke, and U. Nowak, *Phys. Rev. B* **82**, 054415 (2010).
- [31] U. Atxitia, D. Hinzke, O. Chubykalo-Fesenko, U. Nowak, H. Kachkachi, O. N. Mryasov, R. F. Evans, and R. W. Chantrell, *Phys. Rev. B* **82**, 134440 (2010).
- [32] L. Rózsa, U. Atxitia, and U. Nowak, arxiv:1706.01684 (2017).
- [33] G. Finocchio, M. Carpentieri, E. Martinez, and B. Azzerboni, *Appl. Phys. Lett.* **102**, 212410 (2013).
- [34] M. Belmeguenai, J. P. Adam, Y. Roussigné, S. Eimer, T. Devolder, J. Von Kim, S. M. Cherif, A. Stashkevich, and A. Thiaville, *Phys. Rev. B* **91**, 180405(R) (2015).
- [35] H. Yang, A. Thiaville, S. Rohart, A. Fert, and M. Chshiev, *Phys. Rev. Lett.* **115**, 267210 (2015).
- [36] N. Mikuszeit, O. Boulle, I. M. Miron, K. Garello, P. Gambardella, G. Gaudin, and L. D. Buda-Prejbeanu, *Phys. Rev. B* **92**, 144424 (2015).
- [37] C. Schutte, J. Iwasaki, A. Rosch, and N. Nagaosa, *Phys. Rev. B* **90**, 174434 (2014).
- [38] R. Tomasello, M. Ricci, P. Burrascano, V. Puliafito, M. Carpentieri, and G. Finocchio, *AIP Adv.* **7**, 56022 (2017).

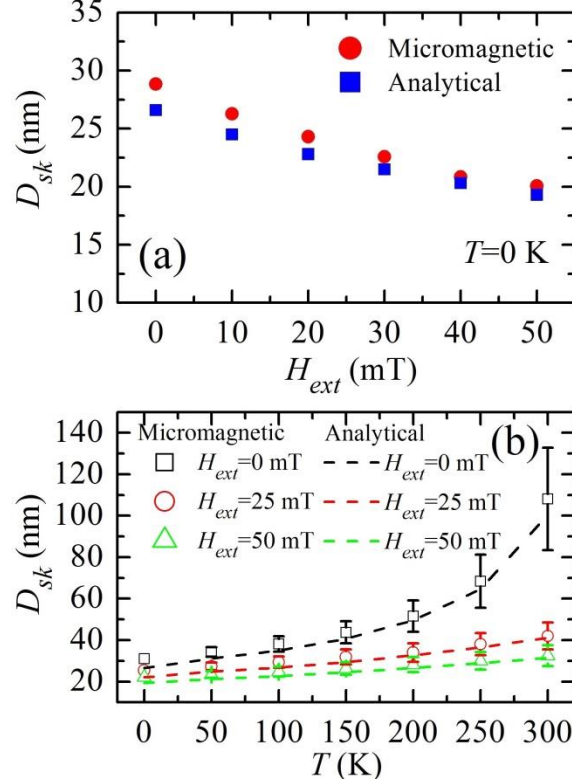


FIG. 1: (a) Skyrmion diameter as a function of the perpendicular external field as computed by micromagnetic simulations (red circles) and by analytical computations based on Eq. (1) (blue squares) at  $T=0$  K. (b) Skyrmion diameter as a function of temperature for three values of the perpendicular external field, as indicated in the legend. The symbols represent the mean value of the skyrmion diameter as obtained by full micromagnetic simulations including thermal fluctuations, where the error bar corresponds to the standard deviation, while the dashed curves are related to the analytical results with scaled values of the macroscopic parameters, using  $\alpha=1.50$ ,  $\beta=1.50$ , and  $\gamma=3.585$ .  $\gamma$  is  $\sim 15\%$  larger than the one derived from atomistic simulations [30].

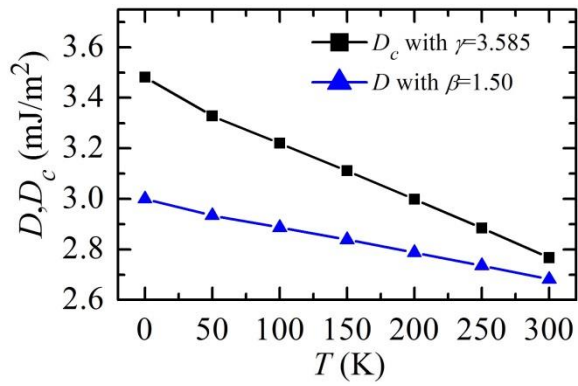


FIG. 2: Comparison of temperature dependences of the scaled DMI parameter  $D$  and the scaled critical DMI parameter  $D_c$  when  $H_{ext}=0$  mT.

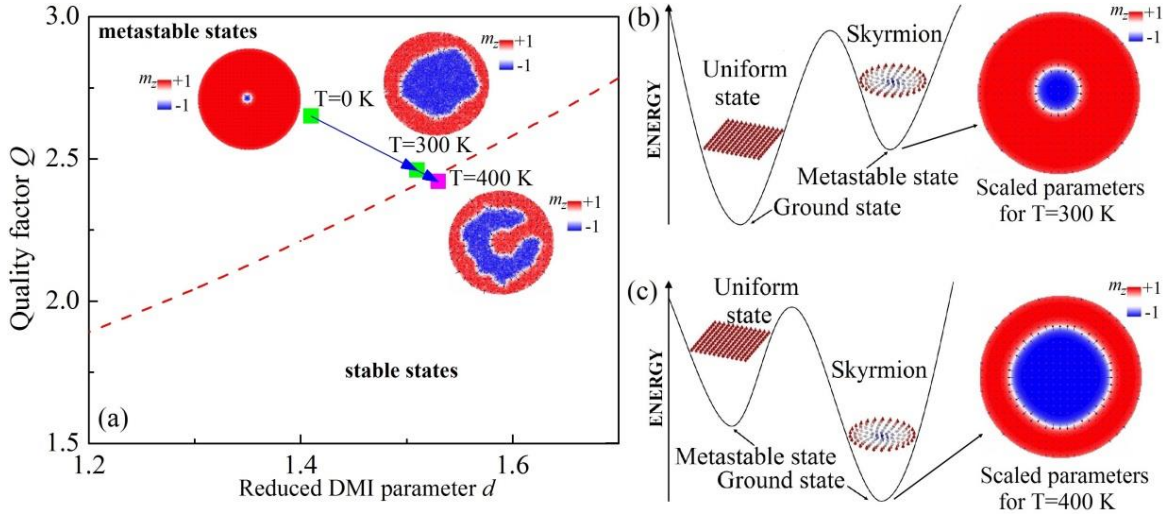


FIG. 3: (a)  $Q$ - $d$  diagram for  $H_{ex}=0$  mT. The green squares indicate the metastable skyrmion states at  $T=0$  K and  $T=300$  K, while the magenta square indicates the stable skyrmion state at  $T=400$  K obtained with our parameters. The dashed red line represents the critical DMI parameter  $D_c$  as defined in Ref. [26]. The blue arrows indicate how the state evolves as a function of temperature. Insets: example of spatial distributions of the magnetization at  $T=0$ ,  $300$  and  $400$  K. Sketch of the energetic profile of the system when the skyrmion corresponds to (b) a metastable state and (c) when it occupies an absolute energy minimum (ground state). Two spatial distributions of the magnetization shown in (b) and (c) refer to deterministic full micromagnetic simulations with scaled values of the parameters for  $T=300$  K and  $T=400$  K, respectively. For all the spatial distributions of the magnetization, a color scale linked to the normalized  $z$ -component of the magnetization is also illustrated.

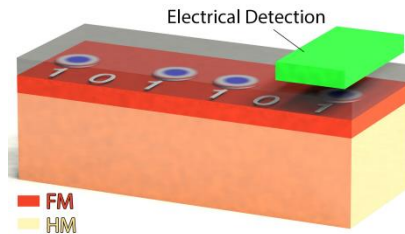


FIG. 4: (a) Sketch of a racetrack memory where the skyrmions (bit '1') are electrically detected below an MTJ (green square).